ELSEVIER

Journal of Alloys and Compounds 408–412 (2006) 468–473

Journal of ALLOYS AND COMPOUNDS

www.elsevier.com/locate/jallcom

Crystal chemistry and electrical conductivity of $Ln_2Eu_2O_3F_6$ (Ln: Nd, La)

Masayuki Takashima [a,*], Susumu Yonezawa [b,1], Jeo-ho Kim [b,1]

[a] *Cooperative Research Center, University of Fukui, 3-9-1 Bunkyo, Fukui 910-8507, Japan*
[b] *Department of Materials Science and Engineering, University of Fukui, 3-9-1 Bunkyo, Fukui 910-8507, Japan*

Received 30 July 2004; received in revised form 30 November 2004; accepted 15 December 2004
Available online 20 June 2005

Abstract

Binary rare-earth metal oxide fluorides $Ln_2Eu_2O_3F_6$ were synthesized by the solid-state reaction between 1 mol Ln_2O_3 (Ln: La, Nd) and 2 mol EuF_3 at 1000–1200 °C in a highly dry atmosphere. $Nd_2Eu_2O_3F_6$ exhibits the oxide ion conductivity of 2.0 S m^{-1} at 500 °C under P_{O_2} = 0.4 Pa, and the transport numbers τO^{2-} was 0.9 at a temperature ranging from 500 to 700 °C. X-ray diffraction Rietveld analysis revealed $Nd_2Eu_2O_3F_6$ was the monoclinic lattice with the crystal parameters a_0 = 0.396 nm, b_0 = 1.13 nm, c_0 = 0.562 nm, b = 134.8°, Z = 1. The structures of $Nd_{2.1}Eu_{1.9}O_3F_6$ and $La_2Eu_2O_3F_6$ were also analyzed as the monoclinic structure (a_0 = 0.397 nm, b_0 = 1.13 nm, c_0 = 0.561 nm, β = 135.0°, Z = 1 for $Nd_{2.1}Eu_{1.9}O_3F_6$ and a_0 = 0.404 nm, b_0 = 1.14 nm, c_0 = 0.574 nm, β = 135.3°, Z = 1 for $La_2Eu_2O_3F_6$). The ionic arrangement was suggested to be not a little disordered in the crystal lattice of $Nd_{2.1}Eu_{1.9}O_3F_6$ and $La_2Eu_2O_3F_6$ in contrast to that in the $Nd_2Eu_2O_3F_6$. The disorder of anionic arrangement in $Nd_{2.1}Eu_{1.9}O_3F_6$ and $La_2Eu_2O_3F_6$ lattice was assumed to result in the lower oxide ion conductivity $Nd_{2.1}Eu_{1.9}O_3F_6$ (σ = 1.0 S m^{-1}, τO^{2-} = 0.9) and $La_2Eu_2O_3F_6$ (σ = 0.8 S m^{-1}, τO^{2-} = 0.7).

Keywords: Binary rare-earth oxide fluoride; Solid electrolyte; Crystal sturucture

1. Introduction

To date, most of the objective compounds to survey oxide ion solid electrolytes were metal complex oxides, such as stabilized zirconia, perovskite-type complex oxides, scheelite-type solid solutions and something like that [1–6]. There was no attempt to synthesize new oxide ion conducting materials based on the idea of anion hybridization of F^- and O^{2-}. Because of the similar ionic size of fluoride and oxide ion, fluoride ion can substitute or incorporate for oxide ion or vacant site in the metal oxides. Therefore, the bond character and the coordination in the crystal structure must be controlled by introducing of F^- into the metal oxides with partially covalent M–O bond [7]. From this concept, the binary rare-earth oxide fluorides, $Ln_2Ln'_2O_3F_6$ in which Ln and Ln′ are different rare earths, have been investigated as oxide ion-conducting solid electrolytes with much higher conductivity than that of stabilized zirconia [8,9]. In this paper, the preparation, crystal structure and electrical conducting properties of binary rare-earth oxide fluorides, $Ln_{2+x}Eu_{2-x}O_3F_6$ (Ln: Nd, La, $x = 0$ and $0.1 < x < 0.6$) have been reported. $Nd_{2+x}Eu_{2-x}O_3F_6$ ($0.1 < x < 0.6$) samples were prepared in order to examine the effect of cationic ratio on the properties.

2. Experimental

$Ln_2Eu_2O_3F_6$ (Ln: Nd, La) are obtained by the solid-state reaction between Ln_2O_3 (Ln: Nd, La) and EuF_3 at a temperature higher than 1000 °C [8–11]. $Nd_{2-x}Eu_{2-x}O_3F_6$ ($0.1 < x < 0.6$) samples were prepared from appropriate mixture of Nd_2O_3, Eu_2O_3 and EuF_3. The anhydrous sesquioxides and trifluorides of rare earths are commercially available in a purity of 99.9–99.99%. Because both EuF_3 and oxide fluoride products are very moisture-sensitive at a tem-

* Corresponding author. Tel.: +81 776 27 8516; fax: +81 776 27 8516.
E-mail addresses: takashima@matse.fukui-u.ac.jp (M. Takashima), yonezawa@matse.fukui-u.ac.jp (S. Yonezawa).
[1] Tel.: +81 776 27 8910; Fax: +81 776 27 8910.

0925-8388/$ – see front matter © 2005 Elsevier B.V. All rights reserved.
doi:10.1016/j.jallcom.2004.12.077

perature higher than 700 °C, all the preparative operations, such as powdering, mixing and firing must be performed in a highly dried atmosphere in addition to sufficient dehydration of starting materials. The compositions of products were analyzed by X-ray fluorescence spectroscopy (Shimadzu: SXF-1100s). The fluoride ion was quantitatively analyzed by means of an ion selective electrode method. The water-soluble sample was prepared by the reaction of oxide fluoride samples with NaOH-melt at 800 °C. The crystal structure was studied by means of X-ray powder diffraction method (Shimadzu XD-3As; Cu Kα, 30 kV, 40 mA; step width, 0.02 (2θ); time constant, 10.0 s). Density was measured by using a helium gas displacement pycnometer (Micromeritics: AccPyc-1330). The X-ray diffraction results were analyzed by computational methods using RIETAN programs [10,11]. The disc samples ($13\phi \times 2$ mm) for the electrical conductivity measurements were prepared by hot pressing at a temperature from 1000 to 1200 °C under 20 MPa in argon. The electrical conductivity has been examined by ac method (EG&G Instruments: Potentiostat 283vs and FRA1120, 3–10 MHz) at a temperature between 400 and 700 °C under a partial pressure of oxygen ranging from 1×10^{-2} to 2×10^{4} Pa [9–12]. The oxide ion transport number was examined by the EMF method using an oxygen gas concentration cell, and the charge-carrying species in $Ln_2Eu_2O_3F_6$ was examined by an electrolysis method [12] and a dc polarization method [13]. The charge-carrying ionic species can be identified using an electrolysis method involving a simple cell with the compressed anode powder mixture of Ni + NiO and the sintered Pt cathode. If the fluoride ion is mobile in the sample compound, the anode mixture should be converted by electrolysis to fluorine containing nickel compounds. On the other hand, if the oxide ion is the charge carrier, consumption of nickel metal in the anode mixture must be detected [12].

3. Results and discussion

By the solid-state reaction between Ln_2O_3 and $Ln'F_3$, two stoichiometrical mono-phases of the rhombohedral $Ln_2Ln'O_3F_3$ and the quasi-tetragonal $Ln_2Ln'_2O_3F_6$ were prepared from an equimolar mixture of Ln_2O_3 and $Ln'F_3$ and a mixture of 1 mol Ln_2O_3 and 2 mol $Ln'F_3$. On the first step of the solid-state reaction, the anion exchange reaction between Ln_2O_3 and $Ln'F_3$ proceeds up to around 600 °C until two kinds of simple rare-earth oxide fluoride, rhombohedral LnOF and tetragonal $Ln'O_xF_{3-2x}$, are formed as intermediates. At a temperature higher than around 900 °C, the mutual diffusion of rare-earth cations between both simple rare-earth oxide fluorides was assumed to proceed to form the binary rare-earth oxide fluoride as shown in Fig. 1.

Although the rare-earth oxide fluorides were first expected to exhibit binary anion conductivity of fluoride and oxide ions, the most of binary rare-earth oxide fluorides were found to indicate mainly oxide ion conductivity. Among them, neodymium europium oxide fluoride, $Nd_2Eu_2O_3F_6$

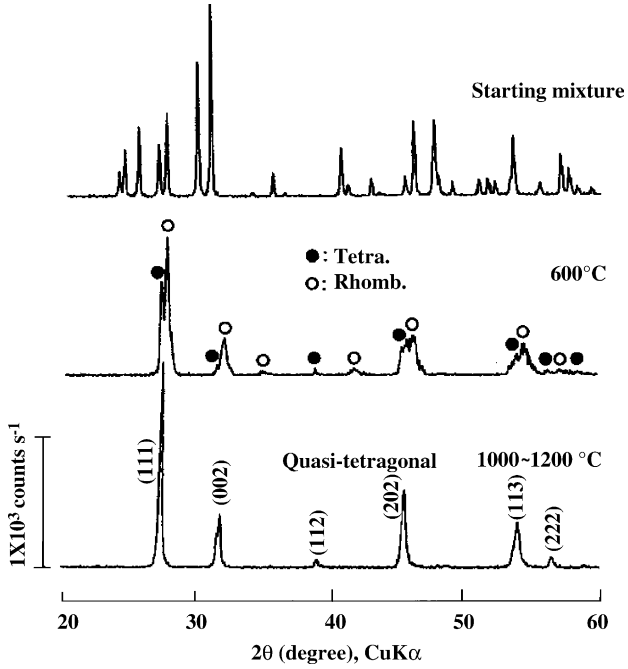

Fig. 1. X-ray diffraction profiles of products obtained from the mixture of 1 mol Nd_2O_3 and 2 mol EuF_3.

gave much higher electrical conductivity than that of yttria-stabilized zirconia [8]. The electrical conductivities of the binary rare-earth oxide fluorides vary not only with the combination of Ln_2O_3 with $Ln'F_3$, but also with the composition of the products. Fig. 2 shows the relationship between the

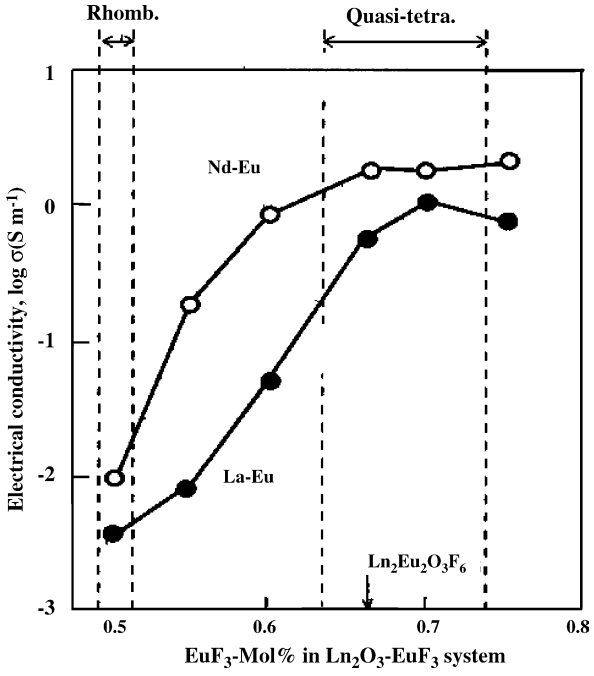

Fig. 2. Relationship between the electrical conductivities of the products obtained from various Ln_2O_3–EuF_3, where Ln = Nd (○) and La (●) systems and nominal compositions of EuF_3. The electrical conductivity was measured at 650 °C under an oxygen partial pressure of 0.13 Pa.

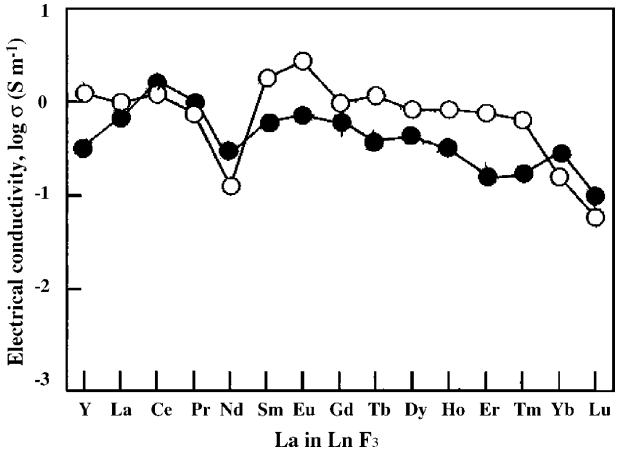

Fig. 3. The electrical conductivities of binary rare-earth oxide fluorides, $Ln_2Ln'_2O_3F_6$, produced from Nd_2O_3–LnF_3 and La_2O_3–LnF_3 systems. The electrical conductivity was measured at 650 °C under an oxygen partial pressure of 0.13 Pa. (◯) Nd_2O_3–LnF_3 system and (●) La_2O_3–LnF_3 system.

electrical conductivity and the nominal composition of EuF_3 for the products obtained from several Ln_2O_3–EuF_3 systems. In both systems, the electrical conductivity steeply increases in the composition range from 50 to 60 mol% EuF_3, where the structural change from the rhombohedral to the quasi-tetragonal takes place. The electrical conduction properties assumed to be affected strongly with the crystal structure varied with the composition. The electrical conductivity of the quasi-tetragonal phase is at least 100 times higher than that of the rhombohedral phase. The electrical conductivities of $Nd_2Ln_2O_3F_6$ and $La_2Ln_2O_3F_6$ are summarized in Fig. 3. Neodymium containing compounds, $Nd_2Ln_2O_3F_6$, except for compounds of Ln: Nd, Yb and Lu, show the much higher electrical conductivities of around 1.0 S m^{-1} than that of $La_2Ln_2O_3F_6$ system. It is worth noting for these elements that these trivalent ions are larger than the limiting size (around 0.09 nm in radius) permitting octa-coordination to both fluoride and oxide anions, and can vary to divalent and/or tetravalent ions except for La^{3+}. The electrical conductivities of $Nd_2Eu_2O_3F_6$ and $La_2Eu_2O_3F_6$ and yttria-stabilized zirconia, YSZ-11: $(ZrO_2)_{0.89}(Y_2O_3)_{0.11}$, measured in dried air evacuated to 1.33×10^{-1} Pa is shown in Fig. 4 in the form of Arrhenius plots. As is evident from this figure, the conductivities of $Nd_2Eu_2O_3F_6$, $Nd_{2.1}Eu_{1.9}O_3F_6$ and $La_2Eu_2O_3F_6$ are higher than that of YSZ. Remarkably, $Nd_2Eu_2O_3F_6$ shows much high conductivity of which the value at 650 °C reaches 5.0 S m^{-1}. This value corresponds to the conductivity of YSZ-11 at 900 °C. The activation energies calculated from the slope of the linear plots of $\ln\sigma$ against reciprocal temperature, $1/T$, are 70 kJ mol^{-1} for $Nd_2Eu_2O_3F_6$, 90 kJ mol^{-1} for $Nd_{2.1}Eu_{1.9}O_3F_6$ and 100 kJ mol^{-1} for $La_2Eu_2O_3F_6$ and YSZ-11. The experimental results on the charge carrier in these compounds determined by the electrolysis method indicate that only the oxide ion is mobile, that is, $Nd_2Ln_2O_3F_6$ can be called an oxide ion-conducting solid electrolyte. The main charge-carrying species of each compound was identified to be the oxide ion and fluoride ion was hardly detected as a charge carrier. As shown in Fig. 5, the oxide ion trans-

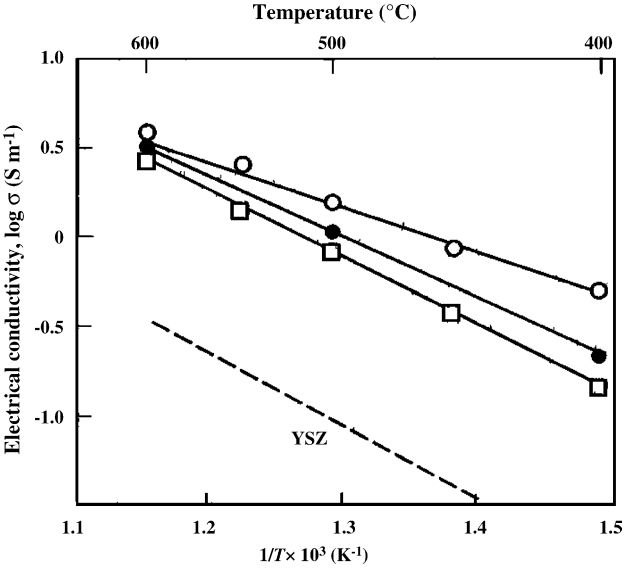

Fig. 4. The electrical conductivities of several binary rare-earth oxide fluorides. (◯) $Nd_2Eu_2O_3F_6$; (●) $Nd_{2.1}Eu_{1.9}O_3F_6$ and (□) $La_2Eu_2O_3F_6$.

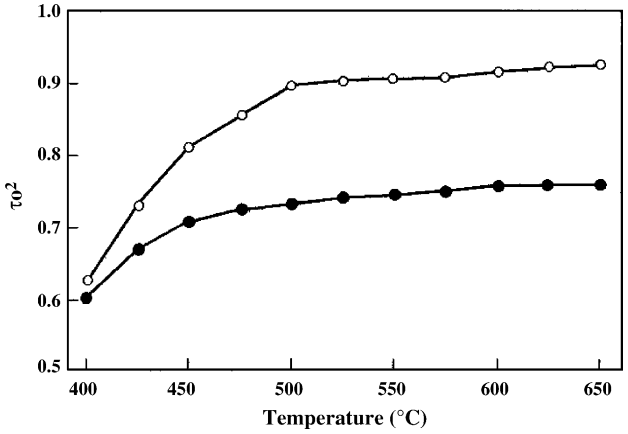

Fig. 5. Oxide ion transport number of $Nd_2Eu_2O_3F_6$(◯) and $La_2Eu_2O_3F_6$(●).

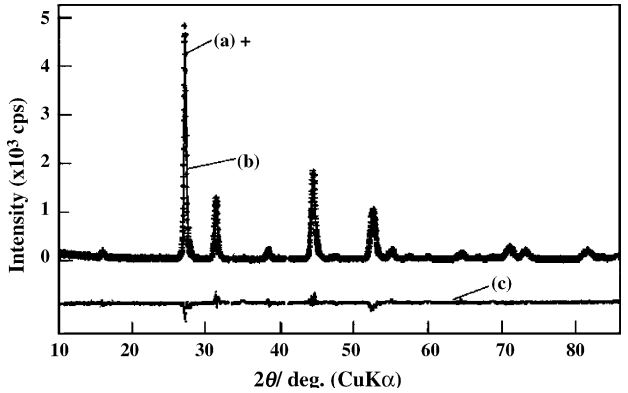

Fig. 6. XRD pattern of $Nd_{2.1}Eu_{1.9}O_3F_6$ and the results of Rietveld refinement: (a) observed; (b) calculated and (c) difference.

port numbers of $Nd_2Eu_2O_3F_6$ and $La_2Eu_2O_3F_6$ are more than 0.9 and 0.7, respectively, at 500–700 °C, where their electron transport numbers were measured to be 0.1 and 0.3, respectively. The transport number of F^- was negligibly small in these cases. This fact has been described in our previous paper [12]. Fig. 6 shows the relationship between the electrical conductivity of $Nd_2Eu_2O_3F_6$ with high oxide ion conductivity at 500 °C and the partial pressure of oxygen. The electrical conduction was confirmed to be due to only the oxide ion because the electrical conductivity was constant under an oxygen partial pressure of more than 0.4 Pa. Both electrical conductivity and oxide ion transport number of $Nd_2Eu_2O_3F_6$ ($\sigma = 2.0\,S\,m^{-1}$, $\tau O^{2-} = 0.9$) at 500 °C was higher than that of $Nd_{2.1}Eu_{1.9}O_3F_6$ ($\sigma = 1.0\,S\,m^{-1}$, $\tau O^{2-} = 0.9$) and $La_2Eu_2O_3F_6$ ($\sigma = 0.8\,S\,m^{-1}$, $\tau O^{2-} = 0.7$) as shown in Figs. 4 and 5. The differences in the oxide ion conductivities among $Nd_2Eu_2O_3F_6$, $Nd_{2.1}Eu_{1.9}O_3F_6$ and $La_2Eu_2O_3F_6$ were discussed from the point of view of the ionic configurations in the crystal lattice. Though many efforts to obtain a single crystal of binary rare-earth oxide fluorides have done, no one has been yet to succeed. In order to determine the crystal structure by using X-ray powder diffraction data, Rietveld analysis have been carried out. Because binary rare-earth oxide fluorides exhibit oxide ion conduction, the structural aspects resulting in the oxide ion conduction have been considered as the background information to simulate the crystal structure. The stoichiometric compounds, $Nd_2Ln_2O_3F_6$ were analyzed by relating to the known structures of simple rare-earth oxide fluorides, such as the tetragonal $Nd_4O_3F_6$ [7,10,11]. The crystal structure analyses of some $Nd_2Ln_2O_3F_6$ (Ln = Ce, Eu, Sm, Gd) compounds with much higher oxide ion conductivity were already finished and their lattice parameters were registered in the powder diffraction file [14]. The main interest here is the analysis of the crystal structure of $Nd_{2.1}Eu_{1.9}O_3F_6$ and $La_2Eu_2O_3F_6$ of which the oxide ion conductivities were somewhat lower than $Nd_2Eu_2O_3F_6$. Because XRD patterns

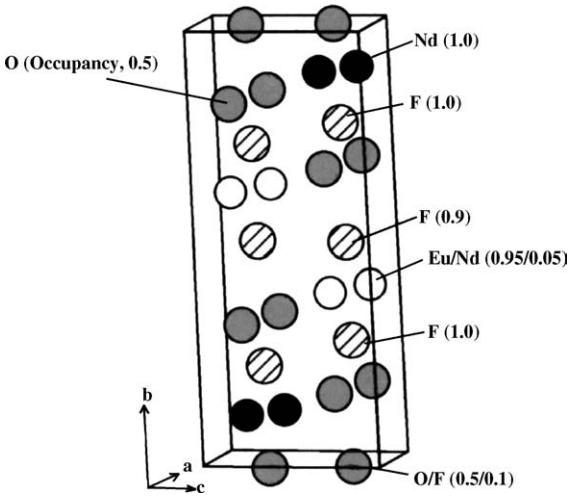

Fig. 7. Unit lattice of $Nd_{2.1}Eu_{1.9}O_3F_6$.

Table 1
Crystallographic data for $Nd_{2.1}Eu_{1.9}O_3F_6$[a]

Atom	Site	x	y	z	Occupancy
Nd	2e	0.0	0.112	0.25	1.0
Nd/Eu	2e	0.0	0.608	0.25	0.05/0.95
O/F	2f	0.5	0.011	0.75	0.5/0.1
F	2f	0.5	0.271	0.75	1.0
F	2f	0.5	0.485	0.75	0.9
F	2f	0.5	0.777	0.75	1.0
O	2e	0.0	0.853	0.25	0.5
O	2e	0.0	0.354	0.25	0.5

[a] Cell parameters $a_0 = 0.397$ nm, $b_0 = 1.13$ nm, $c_0 = 0.561$ nm, $\alpha = 90.0°$, $\beta = 135.0°$, $\gamma = 90.0°$; cell volume $= 1.79 \times 10^{-28}\,m^3$; X-ray density $= 7.00 \times 10^3\,kg\,m^{-3}$; space group, $P1\ 2/c\ 1$ (No. 13); cell contents, $Z = 1$.

of $Nd_{2.1}Eu_{1.9}O_3F_6$ and $La_2Eu_2O_3F_6$ were similar to that of $Nd_2Eu_2O_3F_6$, the Rietveld refinement of crystal structure of these compounds were carried out with the same manner done for $Nd_2Eu_2O_3F_6$ [10], and the results were shown in Fig. 6 and Table 1 for $Nd_{2.1}Eu_{1.9}O_3F_6$ and Fig. 8 and Table 2 for $La_2Eu_2O_3F_6$, respectively. Fig. 7 shows the unit lattice of $Nd_{2.1}Eu_{1.9}O_3F_6$. In the $Nd_2Eu_2O_3F_6$ structure, the ionic arrangement was supposed to be highly ordered. In the case of $Nd_{2.1}Eu_{1.9}O_3F_6$, the Rietveld simulation was done by the condition that the site 2e ($y = 0.608$) was occupied by Eu^{3+} and Nd^{3+} in the ratio of 0.95/0.05. The R_F value, which is the criterion for accuracy of simulation, was 2.69. These values indicate that the Rietveld refinement has been done with enough accuracy to determine the crystal structure. From the results of the Rietveld refinement of $Nd_{2.1}Eu_{1.9}O_3F_6$, the 2e sites at $y = 0.354$ and 0.853 were estimated to be occupied by oxide ion with the occupancy of 0.5. Therefore, the path way for the oxide ion conduction was likely to maintain as so in the $Nd_2Eu_2O_3F_6$. On the other hand, it was suggested that 2f sites at $y = 0.011$ and 0.485 were occupied by O^{2-} and F^- with the occupancy of 0.5/0.1 and F^- with the occupancy of 0.9. Because both fluoride ion and oxide ion occupied at 2f sites with the occupancy less than 1.0 not only conduction of oxide ion but also that of fluoride ion could be considered. This was assumed to be the cause to decline the oxide ion conductivity.

Table 2
Crystallographic data for $La_2Eu_2O_3F_6$[a]

Atom	Site	x	y	z	Occupancy
La/Eu	2e	0.0	0.113	0.25	0.9/0.1
La/Eu	2e	0.0	0.614	0.25	0.1/0.9
O/F	2f	0.5	0.0	0.75	0.5/0.1
F	2f	0.5	0.260	0.75	1.0
F	2f	0.5	0.518	0.75	0.9
F	2f	0.5	0.750	0.75	1.0
O	2e	0.0	0.863	0.25	0.5
O	2e	0.0	0.363	0.25	0.5

[a] Cell parameters $a_0 = 0.404$ nm, $b_0 = 1.14$ nm, $c_0 = 0.572$ nm, $\alpha = 90.0°$, $\beta = 135.3°$, $\gamma = 90.0°$; cell volume $= 1.86 \times 10^{-28}\,m^3$; X-ray density $= 6.68 \times 10^3\,kg\,m^{-3}$; Space group, $P1\ 2/c\ 1$ (No. 13); cell contents, $Z = 1$.

Table 3
Crystal parameters and electrical conductivities of $La_2Eu_2O_3F_6$ and $Nd_2Eu_2O_3F_6$[a]

$Ln_2Ln'_2O_3F_6$	Lattice parameters				Cell volume ($\times 10^{-28}$ m^3)	Density calculated/measured (kg m$^-$)	σ (S m^{-1})[a]	τO^{2-}[b]
	a_0 (nm)	b_0 (nm)	c_0 (nm)	β (°)				
$Nd_2Eu_2O_3F_6$	0.396^1	1.13^2	0.563^2	134.8	1.79	7.00/6.99	2.2	0.9
$Nd_{2.1}Eu_{1.9}O_3F_6$	0.396^8	1.13^0	0.561^5	135.0	1.79	7.00/7.00	1.0	0.8
$Nd_{2.3}Eu_{1.7}O_3F_6$	0.396^9	1.13^3	0.562^7	135.0	1.79	6.96/6.97	0.7	–
$Nd_{2.5}Eu_{1.5}O_3F_6$	0.397^1	1.13^5	0.562^3	134.8	1.80	6.93/6.94	0.5	–
$La_2Eu_2O_3F_6$	0.404	1.14	0.572	135.3	1.86	6.68/6.70	0.8	0.7

The superscript number is the standard deviation of each value.
[a] Electrical conductivity was measured at 500 °C under 5.3 Pa oxygen.
[b] Oxide ion transport number was measured at 500 °C.

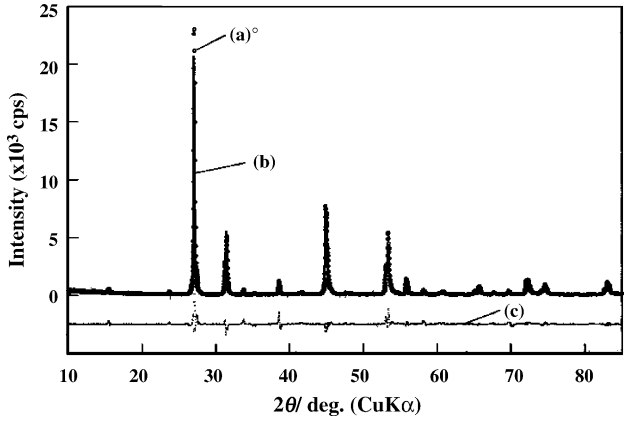

Fig. 8. XRD pattern of $La_2Eu_2O_3F_6$ and the results of Rietveld refinement: (a) observed; (b) calculated and (c) difference.

In case of $La_2Eu_2O_3F_6$, the Rietveld refinements revealed that 10% of La^{3+} at 2e ($y = 0.1134$) site and 10% of Eu^{3+} at 2e ($y = 0.6140$) site were mutually exchanged. A disordering in the anion arrangement was caused by this disordering in the cation arrangement. The R_F value reached 6.78, which was a little too large to determine; finally, the crystal structure compared with the values of 2.69 for $Nd_{2.1}Eu_{1.9}O_3F_6$ and 3.03 for $Nd_2Eu_2O_3F_6$ [10]. It may arise from the presence of $LaEuO_2F_2$ and $LaEuO_3$ in the sample as the impurities resulting from pyrohydrolysis. In any case, it is certain that the ionic arrangement in $La_2Eu_2O_3F_6$ tends to be disordered rather than that in $Nd_{2.1}Eu_{1.9}O_3F_6$. As the results of $Nd_{2.1}Eu_{1.9}O_3F_6$, the 2e sites occupied by oxide ion were maintained to be the occupancy of 0.5, and the 2f sites layered at $y = 0.0$ plane were occupied partially by fluoride ion in the lattice of $La_2Eu_2O_3F_6$. The crystal parameters and the electrical conductivities of $Nd_2Eu_2O_3F_6$, $Nd_{2+x}Eu_{2-x}O_3F_6$ and $La_2Eu_2O_3F_6$ were summarized in Table 3.

4. Conclusion

$Nd_2Eu_2O_3F_6$ and $La_2Eu_2O_3F_6$ were synthesized by the solid-state reaction between 1 mol Ln_2O_3 (Ln; La, Nd) and 2 mol EuF_3 at 1000–1200 °C in highly dried argon. $Nd_{2+x}Eu_{2-x}O_3F_6$ ($0.1 < x < 0.6$) samples were also prepared to consider the effects of cation arrangement in crystal lattice on the electrical conductivity. $Nd_2Eu_2O_3F_6$ gave the conductivity of 2.0 S m^{-1} at 500 °C under $P_{O_2} = 0.4$ Pa, and the transport numbers of oxide ion and electron were measured to be 0.9 and less than 0.05, respectively, at a temperature ranging from 500 to 700 °C. As the results of X-ray powder diffraction-Rietveld analysis, the crystal structure of $Ln_2Eu_2O_3F_6$ and $Nd_{2+x}Eu_{2-x}O_3F_6$ were analyzed to be the monoclinic lattice. The crystal parameters of $Nd_2Eu_2O_3F_6$ were calculated to be $a_0 = 0.396$ nm, $b_0 = 1.13$ nm, $c_0 = 0.562$ nm, $b = 134.8°$, $Z = 1$. The crystal structure of $Nd_{2.1}Eu_{1.9}O_3F_6$ and $La_2Eu_2O_3F_6$ were determined to be also the monoclinic structure ($a_0 = 0.397$ nm, $b_0 = 1.13$ nm, $c_0 = 0.561$ nm, $\beta = 135.0°$, $Z = 1$ for $Nd_{2.1}Eu_{1.9}O_3F_6$ for $Nd_{2.1}Eu_{1.9}O_3F_6$ and $a_0 = 0.404$ nm, $b_0 = 1.14$ nm, $c_0 = 0.574$ nm, $\beta = 135.3°$, $Z = 1$ for $La_2Eu_2O_3F_6$). The ionic arrangement in their crystal lattice was found to be not a little disordered in the $Nd_{2.1}Eu_{1.9}O_3F_6$ and $La_2Eu_2O_3F_6$ in contrast to that in the $Nd_2Eu_2O_3F_6$ with a highly ordered ionic arrangement. It was assumed that the disorder of anionic arrangement in $Nd_{2.1}Eu_{1.9}O_3F_6$ or $La_2Eu_2O_3F_6$ lattice resulted in the lower oxide ion conductivity $Nd_{2.1}Eu_{1.9}O_3F_6$ ($\sigma = 1.0$ S m^{-1}, $\tau O^{2-} = 0.8$) and $La_2Eu_2O_3F_6$ ($\sigma = 0.8$ S m^{-1}, $\tau O^{2-} = 0.7$). It was assumed that the disorder of ionic arrangement in $La_2Eu_2O_3F_6$ resulted in the lower oxide conductivity $La_2Eu_2O_3F_6$ ($\sigma = 0.8$ S m^{-1}, $\tau O^{2-} = 0.7$ at 500 °C) than that of $Nd_2Eu_2O_3F_6$.

References

[1] N.Q. Monh, T. Takahashi, Science and Technology of Ceramic Fuel Cell, Elsevier, Amsterdam, 1995.
[2] A. Kvist, in: J. Hladik (Ed.), Physics of Electrolytes, vol. 1, Academic Press, London, 1972 (Chapter 8).
[3] K.R. Kendal, C. Navas, J.K. Thomas, H. Loye, Solid State Ionics 82 (1995) 215.
[4] T. Ishihara, h. Masuda, Y. Takita, J. Am. Chem. Soc. 116 (1994) 3801.
[5] A. Petric, P. Haung, Solid State Ionics 92 (1996) 113.
[6] T. Esaka, T. Ikebe, M. Kamata, Solid State Ionics 76 (1995) 237.
[7] B.L. Chamberland, in: P. Hagenmuller (Ed.), Inorganic Solid Fluorides, Academic Press Inc., Orland, 1985 (Chapter 5).
[8] M. Takashima, G. Kano, Solid State Ionics 23 (1987) 99.
[9] M. Takashima, S. Yonezawa, K. Horita, K. Ohwaki, H. Takahashi, J. Mater. Chem. 6 (1996) 795.

[10] M. Takashima, S. Yonezawa, Y. Ukuma, J. Fluorine Chem. 87 (1998) 229.
[11] M. Takashima, S. Yonezawa, T. Tanioka, Y. Nakajima, M. Leblanc, Solid State Sci. 2 (2000) 71–76.
[12] M. Takashima, J. Fluorine Chem. 105 (2000) 249–256.
[13] C. Wagner, Adv. Electrochem. Eng. 4 (1966) 1.
[14] Powder diffraction file (JCPD), 50-1779, 50-1782, 50-1783, International Centre for Diffraction Data (2000).